JOURNAL OF ENVIRONMENTAL SCIENCES 95 (2020) 49–57

Available online at www.sciencedirect.com

ScienceDirect

www.elsevier.com/locate/jes

JES JOURNAL OF ENVIRONMENTAL SCIENCES

www.jesc.ac.cn

Relationships between chemical elements of $PM_{2.5}$ and O_3 in Shanghai atmosphere based on the 1-year monitoring observation

Junyang Zeng[1], *Luying Zhang*[1], *Chuanhe Yao*[1], *Tingting Xie*[1], *Lanfang Rao*[1], *Hui Lu*[2], *Xinchun Liu*[2,*], *Qingyue Wang*[3], *Senlin Lu*[1,*]

[1] *School of Environmental and Chemical Engineering, Shanghai University, Shanghai 200444, China*
[2] *Institute of Desert Meteorology, China Meteorological Administration, Urumqi 83002, China*
[3] *School of Science and Engineering, Saitama University, Saitama 338-8570, Japan*

ARTICLE INFO

Article history:
Received 10 September 2019
Revised 3 March 2020
Accepted 17 March 2020
Available online 29 April 2020

Keywords:
Shanghai $PM_{2.5}$
O_3
Chemical elements

ABSTRACT

Mass level of fine particles ($PM_{2.5}$) in main cities in China has decreased significantly in recent years due to implementation of Chinese Clean Air Action Plan since 2013, however, O_3 pollution is getting worse than before, especially in megacities such as in Shanghai. In this work, O_3 and $PM_{2.5}$ were continuously monitored from May 27, 2018 to March 31, 2019. Our data showed that the annual average concentration of $PM_{2.5}$ and O_3 (O_3-8 hr, maximum 8-hour moving average of ozone days) was 39.35 ± 35.74 and 86.49 ± 41.65 μg/m^3, respectively. The concentrations of $PM_{2.5}$ showed clear seasonal trends, with higher concentrations in winter (83.36 ± 18.66 μg/m^3) and lower concentrations in summer (19.85 ± 7.23 μg/m^3), however, the seasonal trends of O_3 were different with 103.75 ± 41.77 μg/m^3 in summer and 58.59 ± 21.40 μg/m^3 in winter. Air mass backward trajectory, analyzing results of potential source contribution function model and concentration weighted trajectory model implied that pollutants from northwestern China contributed significantly to the mass concentration of Shanghai $PM_{2.5}$, while pollutants from areas of eastern coastal provinces and South China Sea contributed significantly to the mass level of ozone in Shanghai atmosphere. Mass concentration of twenty-one elements in the $PM_{2.5}$ were investigated, and their relationships with O_3 were analyzed. Mass level of ozone had good correlation with that of Ba ($r = 0.64, p < 0.05$) and V ($r = 0.30, p > 0.05$), suggesting vehicle emission pollutants contribute to the increasing concentration of ozone in Shanghai atmosphere.

Introduction

Particulate matters (PMs) were widely studied due to their environmental effects and various harmful effects on human health in the last decades (Lu et al., 2008, 2011). Based on their aerodynamic diameter (D), particulate matters can be divided into coarse particles (PM_{10}, $D \leq 10$ μm), fine particles ($PM_{2.5}$, $D \leq 2.5$ μm) and ultrafine particles ($D \leq 0.1$ μm). Due to the fine particles have smaller particle size and larger surface area per unit mass compared with that of coarse particles, various harmful gasses and heavy metals can be easily adsorbed on $PM_{2.5}$. Shanghai, the biggest city in China, has a fleet of over 3.6 million vehicles and a population of over 2400 million permanent residents, which results in high emis-

* Corresponding authors.
E-mails: liuxch@idm.cn (X. Liu), senlinlv@staff.shu.edu.cn (S. Lu).

https://doi.org/10.1016/j.jes.2020.03.043
1001-0742/

sions of NO_x, volatile organic compounds (VOCs), and PMs to the atmosphere from industrial and commercial activities (Xu et al., 2019). Previous studies showed that mass concentration of $PM_{2.5}$ in Shanghai atmosphere showed seasonal variation with much higher values in winter and spring, lower values in summer, and the lowest in autumn (Lu et al., 2008). Its annual average concentration (from 2013 to 2015) of $PM_{2.5}$ was 52.7 μg/m^3 (Wang et al., 2019). The $PM_{2.5}$ was associated with all-cause mortality and respiratory disease mortality in Shanghai (Wang et al., 2019). Additionally, $PM_{2.5}$ chemical components (such as NH_4NO_3 and $(NH_4)_2SO_4$) were contributed to the light extinction efficient in Shanghai (Zhou et al., 2016), and sources of $PM_{2.5}$ was mainly contributed by secondary aerosol and vehicle exhaust (Li et al., 2019a).

O_3 is a secondary pollutant formed via photochemical reactions among precursors including nitrogen oxides (NO_x) and VOC under solar radiation. Ground-level ozone is prescribed as one of six criteria air pollutants by the United States Environmental Protection Agency (US EPA) (Zhang et al., 2019a, 2019b; Zhao et al., 2018), and regarded as a threat to human health (https://www.who.int/airpollution/en/), vegetation (Dolker et al., 2019), and infrastructure.

Mass level of fine particles ($PM_{2.5}$) in main cities in China has decreased significantly in recent years due to implementation of Chinese Clean Air Action Plan since 2013, however, reductions in $PM_{2.5}$ and O_3 were not apparent over the last years (Li et al., 2019b). O_3 pollution is getting worse than before, especially in megacities such as Beijing and Shanghai. The days that O_3 as the major pollutant already outnumbered PM_{10} (Xu et al., 2019). According to the Shanghai Environmental Bulletin (2018), the 90th percentile of the average of maximum daily 8-hr ozone concentration (O_3-8 hr) was 84.47 ppbV and increased 10.4% in 2017 compared with that in 2016. Li et al. (2019b) reported that O_3 pollution in Shanghai, was mainly caused by the joint effect of local to regional precursor emissions combined with super-regional O_3 transport. Shu et al. (2019) demonstrated that super-regional transport was prominent (30.3%–63%) in O_3 pollution in Shanghai. However, most of the studies focused on specific ozone episodes, thus, the results were applicable for these specific cases. Until now, reports on long term observation of O_3 and $PM_{2.5}$, especially, relationship between O_3 and chemical elements in the $PM_{2.5}$ has not been reported. Therefore, our objective was to investigate potential sources and the inter-relationships between the chemical elements in $PM_{2.5}$ and O_3 basing on long term observation. We tried to provide fundamental data for the prevention and control measurement of $PM_{2.5}$ and O_3.

1. Methodology

1.1. Sampling site and monitoring methods

Sampling site was located on the roof of a teaching building in the campus of Shanghai University (31°19′0″N, 121°23′25″E) and the height was ~15 m above the ground level. $PM_{2.5}$ samples were collected by using of $PM_{2.5}$ sampler (FLD-1, SIBATA, Japan) with a flow rate of 1.7 L/min from 12:00 at noon and lasted for about 72 hr. 103 samples were collected on quartz fiber filters (SIBATA Company, with diameter of 47 mm). All filters were baked at 450°C for 6 hr and kept in aluminum foil envelopes before sampling. The filters were weighted before and after sampling by a microbalance (balance sensitivity: ±0.001 mg) under the condition of constant temperature (25°C) and relative humidity (40%). Then all filters were stored in the freezer at −20°C until chemical analysis. Ozone analyzer (Thermo 49i, ThermoFisher Scientific, USA) was used to continuously and automatically monitor ozone concentration in ambient air. The O_3-8 hr value was calculated from the on-line data monitored by zone analyzer (Thermo 49i, ThermoFisher Scientific, USA). Parameters of the ozone analyzer are listed in Appendix A Table S1.

1.2. Backward trajectory model and clustering analysis

HYSPLIT model (http://www.noaa.gov) was employed to analysis the air backward trajectories during the monitoring period. The model was run at starting times of 04:00, 10:00, 16:00 and 22:00 coordinated universal time (UTC) (12:00, 18:00, 00:00 and 06:00 for local time, respectively) every day during sampling period. The duration of the calculation was 72 hr, and the height was 500 m above ground level. In this study, the used criterions of the $PM_{2.5}$ and O_3-8 hr were 75 and 160 μg/m^3, respectively.

1.3. Potential source contribution function (PSCF) and concentration weighted trajectory (CWT)

Potential source contribution function (PSCF) and concentration weighted trajectory (CWT) were analyzed by using software TrajStat to identify spatial sources of $PM_{2.5}$ and O_3 (Zhao et al., 2019a, 2019b). The PSCF values for $i \times j$ grid cells in the domain were calculated by counting the trajectory segment endpoints terminating within each cell. By defining the number of endpoints that falls in the ijth cell as n_{ij} and the number of endpoints that corresponds to pollutant concentrations larger than an arbitrarily set criterion when arriving at the receptor site in the same grid cell as m_{ij}, the PSCF value for the ijth cell is defined as (Ashbaugh et al., 1985):

$$\mathrm{PSCF}_{ij} = \frac{m_{ij}}{n_{ij}}$$

The PSCF value represents a conditional probability describing the potential contribution of a grid cell to the high pollutant loadings at the receptor site. In order to reduce the uncertainty in cells by decreasing the effect of small n_{ij} value, the value of PSCF was multiplied with an arbitrary weighting function W_{ij} as following (Wang et al., 2009):

$$W_{ij} = \begin{cases} 0.7 & 20 < n_{ij} < 80 \\ 0.42 & 10 < n_{ij} < 20 \\ 0.17 & n_{ij} \le 10 \end{cases}$$

The PSCF value only gives the spatial distribution of potential emission sources without information on the relative significance of the source regions. To compensate the limitation, a concentration-weighted trajectory (CWT) method developed by Hsu et al. (2003) was used to calculate the trajectory weighted concentration. The studied domain was in the range of 10°N to 60°N and 80°E to 150°E with the resolution of 0.5° × 0.5°, which contained almost all regions overlaid with entire airflow transport pathways. The CWT could be defined as:

$$C_{ij} = \frac{k}{\sum_{k=1}^{M} \tau_{ijk}} \sum_{k=1}^{M} C_k \tau_{ijk}$$

where, C_{ij} was the CWT value in the ijth cell, k was the index of the trajectories that passed the ijth cell, M was the total number of the trajectories, C_k was the concentration of trajectory l, and τ_{ijk} was the number of points falling in the ijth cell by trajectory k. A high CWT value in a cell implied that air parcels traveling over the cell would be associated with high

Table 1 – Sampling information of the selected PM2.5 samples.

No.	Summer	Autumn/North	Winter	Spring	Northwest
1	2018/06/26–2018/06/29	2018/11/07–2018/11/10	2019/01/11–2019/01/14	2019/03/17–2019/03/20	2018/12/02–2018/12/05
2	2018/06/29–2018/07/02	2018/11/10–2018/11/13	2019/01/14–2019/01/17	2019/03/20–2019/03/23	2018/12/05–2018/12/08
3	2018/07/02–2018/07/05	2018/11/13–2018/11/16	2019/01/17–2019/01/20	2019/03/23–2019/03/26	2018/12/17–2018/12/20
4	2018/07/05–2018/07/08	2018/11/16–2018/11/19	2019/01/20–2019/01/23	2019/03/29–2019/04/01	2018/12/20–2018/12/23
5	2018/07/08–2018/07/11	2018/11/19–2018/11/22	2019/01/23–2019/01/26	2019/04/01–2019/04/04	2018/12/23–2018/12/26

concentrations at the receptor station. The weighting function described above was also used in the CWT analyses. Weighted PSCF and CWT (WPSCF and WCWT) were used in the results section.

1.4. *Chemical elements in $PM_{2.5}$*

Based on the air mass trajectory and seasons, 25 samples were selected from the total 103 samples for chemical elements analysis. The 25 samples were divided into six types of samples i.e. spring samples, summer samples, autumn samples, winter samples, north samples (the air mass from north direction) and northwest samples (the air mass from northwest direction). It was worth noting that the autumn samples were also north samples. The selected samples' information is shown in Table 1.

Chemical analyses of the particles were carried out using an Epsilon 4 energy dispersive X-ray fluorescence spectrometer (EDXRF, Malvern Panalytical, Netherlands). Chemical elements from sodium (Na) to americium (Am) could be analyzed by using of the EDXRF. A blank quartz filter was used as a control in the experiment.

1.5. *Statistical analysis*

Data of mass level of $PM_{2.5}$ and O_3 were analyzed with GraphPad InStat software (Version 5.0, GraphPad Software, USA). Statistical significance between O_3 and chemical elements was carried out by using one-way analysis of variance with post hoc Tukey's pairwise comparisons.

2. Results and discussion

2.1. *Mass concentrations of $PM_{2.5}$ and ozone*

Fig. 1 shows the daily average mass concentration of $PM_{2.5}$ and O_3 at the sampling site during the sampling period. The mass concentration of $PM_{2.5}$ ranged from 6.04 to 220.74 μg/m^3, with an average of 39.35 ± 35.74 μg/m^3. Among the whole sampling days (293 days), the $PM_{2.5}$ mass concentration in 44 days exceeded the Chinese pollution standard of 75 μg/m^3 ($PM_{2.5}$ polluted day), and the polluted days ratio was 15.02%. High $PM_{2.5}$ concentration was found in autumn and winter, the high $PM_{2.5}$ concentration (55.52 ± 40.82 μg/m^3) was found from November 2018 to March 2019, with a polluted days percentage of 27.97%. The low $PM_{2.5}$ concentration with the average of 22.08 ± 15.85 μg/m^3 was found in spring and in summer. During this period, only two days could be identified as $PM_{2.5}$ polluted days (on the 5th June, 91.21 μg/m^3; on the 24th October, 78.00 μg/m^3) (detail information is presented in Appendix A Table S2).

The variation of O_3-8 hr at the sampling site ranged from 6.27 to 252.91 μg/m^3, with an average of 86.49 ± 41.65 μg/m^3 during the sampling period. The variation of O_3-8 hr value was different with that of $PM_{2.5}$, showing high concentration in spring and summer, and low concentration in autumn and winter (November 2018 to February 2019). A period of low O_3-8 hr with the average of mass level (58.59 ± 21.40 μg/m^3), and high O_3-8 hr level (103.75 ± 41.77 μg/m^3) was found in May to October 2018 and March 2019. The percentage that O_3-8 hr polluted days exceeded the Chinese pollution standard (160 μg/m^3) was varied from 0% to 8.84%. It is worth noting that the variety of mass level of $PM_{2.5}$ and O_3 was similar during the sampling data from 25th May to 26th October 2018, coefficient between mass level of $PM_{2.5}$ and O_3 was 0.47, suggesting the mass concentration of the two kinds pollutant have a similar variation. This phenomenon was also reported by Zhao et al. (2015). However, the coefficient between mass level of $PM_{2.5}$ and O_3 was 0.18 from 27th October to 31st March 2018, reflecting the variation of the mass concentration of $PM_{2.5}$ and O_3 was different.

2.2. *Cluster analysis*

The back trajectories were clustered into four groups based on air mass directions (Table 2): Cluster 1 was from east, Cluster 2 was from north, Cluster 3 was from southwest and Cluster 4 was from northwest (Fig. 2). Cluster 1 accounted 37.8% among all the analyzed trajectories, while Cluster 2, Cluster 3 and Cluster 4 accounted 27.2%, 12.5% and 22.5% respectively. The cluster 1 originated from eastern sea surface. Cluster 2 originated from Hebei and Liaoning provinces. Cluster 3 was from Guangdong Province and the pathway traveled through Zhejiang and Fujian Province. Cluster 4 arrived in Shanghai after travelling through Mongolia, Hebei and Shandong Province.

The number of trajectories assigned to Cluster 1 was the highest (37.8%) and the air masses associated with this cluster led to the lowest $PM_{2.5}$ loading (30.67 ± 31.01 μg/m^3) among all four clusters. Most trajectories in the Cluster 1 were relatively clean and came from marine. Cluster 2 with high $PM_{2.5}$ concentration (47.40 ± 45.44 μg/m^3) was a short-range trajectory. Most trajectories of Cluster 3 originated from economically developed areas such as Zhejiang province, Fujian province, Guangdong province, and the air masses associated with this cluster led to relatively low (35.28 ± 23.35 μg/m^3) of $PM_{2.5}$. The highest average $PM_{2.5}$ concentration (48.44 ± 32.20 μg/m^3) associated with Cluster 4 (from the northwest to Shanghai) was found in winter and spring. Zhao et al. (2015) reported that the air masses originated from these regions, such as the Inner Mongol and the Gobi desert might carry dust and mixed with other pollutants (SO_x, NO_x) emitted from combustion on their pathways (including Shanxi and Hebei Province, where large amounts of coal were used for heating) and arrived at Shanghai, and led to high mass concentration of $PM_{2.5}$.

It is worth noting that the mean concentration of Cluster 3, polluted trajectory mean value and polluted ratio of Cluster 3 were much higher than other clusters. Because the ozone near the ground surface was mainly formed by some complex

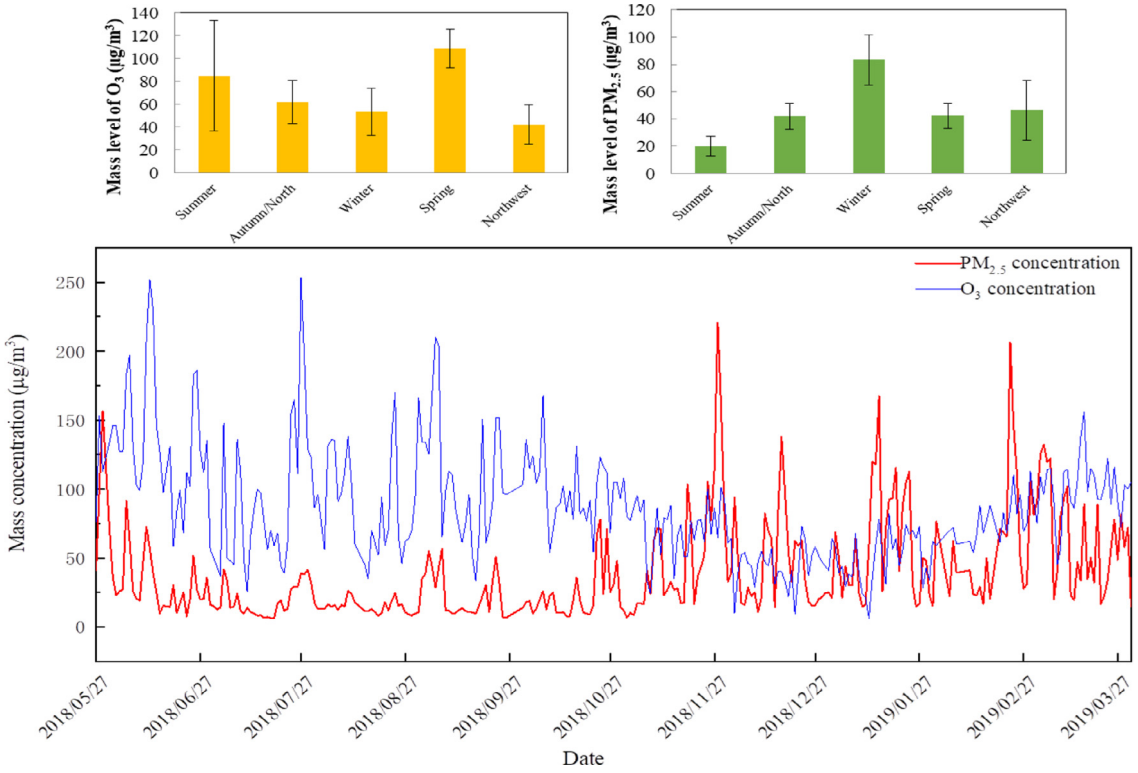

Fig. 1 – Variations of daily $PM_{2.5}$ concentration and daily O_3-8 hr concentration during sampling period. Histograms were seasonal average value of $PM_{2.5}$ and O_3-8 hr.

Table 2 – Cluster statistics of 4 clusters with different air directions.

Cluster number	Trajectory number	Mean concentration of trajectories	Standard deviation of trajectories	Polluted trajectory number	Polluted trajectory ratio	Mean concentration of polluted trajectories	Standard deviation of polluted trajectories
1	436	30.67	31.01	50	11.5%	103.68	25.66
2	313	47.40	45.44	62	19.8%	124.48	41.53
3	144	35.28	23.35	13	9.0%	92.98	4.25
4	259	48.44	32.20	51	19.7%	99.73	22.28
Total	1152	39.79	35.91	176	15.3%	109.07	32.65

chemical reactions between nitrogen oxides (NO_x) and volatile organic compounds (VOCs) from sources such as motor vehicles and industry (Wang et al., 2017). Geng et al. (2008) reported that automobiles played important roles in the O_3 formation in the city of Shanghai, therefore, pollutant sources on this cluster might largely contributed to the increasing mass level of O_3. Additionally, in summer, Cluster 3 traveled through the developed coastal provinces (Guangdong, Fujian and Zhejiang provinces) with the huge traffic flow, and then the ozone precursors such as NO_x and VOCs from automobile exhaust and industrial emissions were higher than that in other regions (Zhao et al., 2015). Therefore, the high concentrations of NO_x and VOCs, high temperature and strong light irradiation triggered the higher ozone mass concentration in the areas than in other regions.

2.3. *PSCF and CWT*

Spatial distributions of $PM_{2.5}$ and ozone potential sources obtained by using the software of TrajStat are shown in Figs. 3 and 4, respectively. The higher CWT and PSCF values indicated more remarkable potential source regions, which were represented by the color of legend. The deeper in red represented the higher level of pollution while the deeper in blue was on the opposite.

Fig. 3 showed that the larger values of PSCF were mainly concentrated in Shaanxi Province, Ningxia Hui Autonomous Region, Gansu Province, western Inner Mongolia and northeastern Xinjiang. The larger values of CWT were mainly concentrated in Jiangsu province, Shanxi province, Shaanxi province, Ningxia Hui Autonomous Region, Gansu province, western Inner Mongolia and northeastern Xinjiang. Weak CWT values were mainly found in sea surface in eastern Shanghai. In general, both PSCF and CWT algorithm indicated Shanxi province, Gansu province, Ningxia Hui, Autonomous Region, Inner Mongolia, and northeastern Xinjiang as major potential source areas of $PM_{2.5}$.

The spatial distributions of potential source areas and transport pathways of ozone are illustrated in Fig. 4. The larger PSCF and CWT value was mainly found in Zhejiang province,

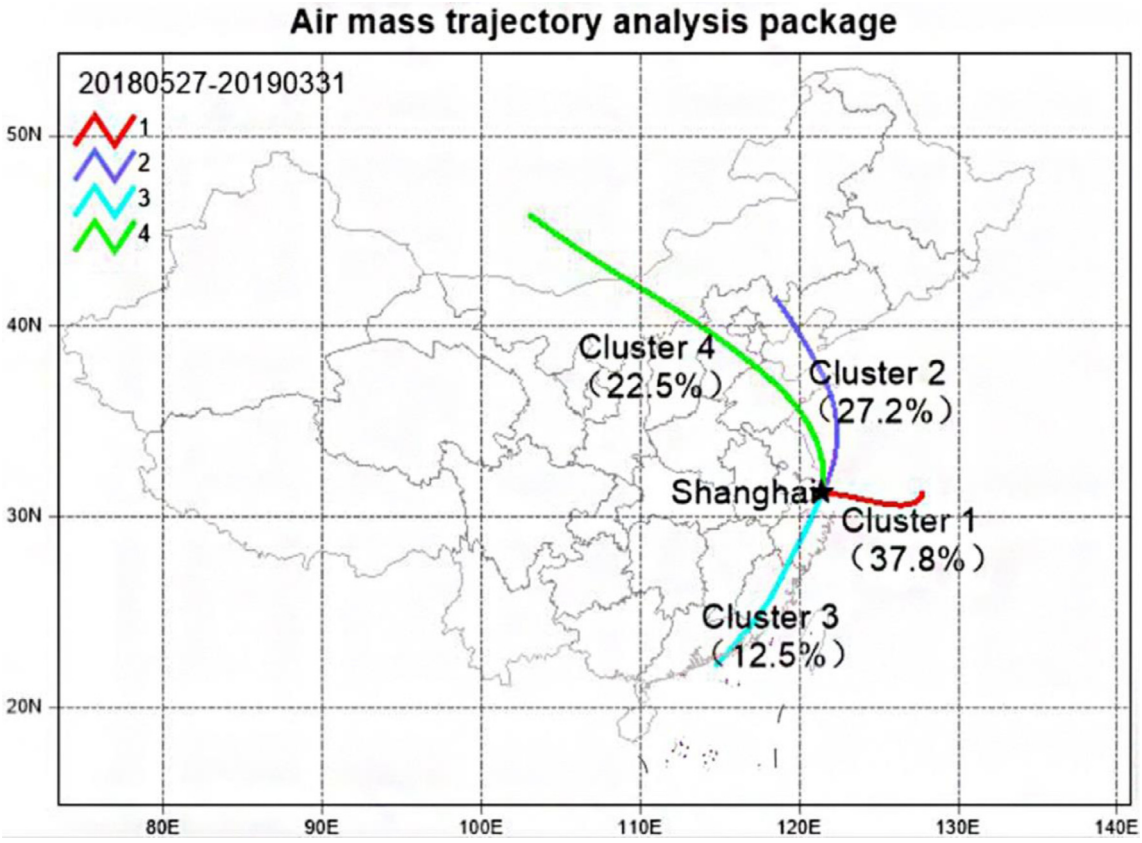

Fig. 2 – Air mass backward trajectories for Shanghai during the sampling time from 27th May 2018 to 31th March 2019 (No. GS (2016) 1585 (http://bzdt.ch.mnr.gov.cn/index.html)).

Fujian province, Guangdong province and South China Sea, while moderate CWT value occurred in the northeast region, such as in Jilin, Liaoning province.

2.4. *Chemical compositions of $PM_{2.5}$*

Twenty-one elements (Na, Mg, Al, Si, P, S, Cl, K, Ca, Ti, V, Cr, Mn, Fe, Ni, Cu, Zn, Br, Sr, Ba, Pb) in $PM_{2.5}$ were investigated in this study. The mean concentrations of the chemical elements are listed in the Table 3.

X-ray fluorescence spectrometer (XRF) data showed that total mass concentrations of analyzed chemical elements in Shanghai $PM_{2.5}$ collected in spring, summer, autumn and winter were 3149.71, 12483.05, 16325.44, and 4479.63 ng/m^3, respectively. It is note that average mass concentration of $PM_{2.5}$ in winter was the highest (83.36 ± 18.56 μg/m^3) among the four seasonal samples, however, mass level of the total chemical elements in winter samples was relative lower than that of summer and autumn samples. The main reason might be there were lots of unidentified fractions by XRF, such as Si, C, in the $PM_{2.5}$.

Among the analyzed elements, calcium was the most abundant element. It's highest mass concentration (6475.33 ± 797.78 ng/m^3) was found in the samples came from Northwest in winter, and the lowest (385.87 ± 299.66 ng/m^3) was in spring samples. The high level of Ca in summer and in autumn $PM_{2.5}$ was probably caused by Shangda road maintenance activities, which could coarse particles suspended in the air.

K was regarded as a marker for biomass burning. The highest mass level of K (2956.94 ± 2415.64 ng/m^3) was found in autumn samples, this data agreed with previous reports (Wang et al., 2013; Zhao et al., 2015). It is worth noting that the mean concentration of K in autumn samples is much higher than that in other seasons (4.7, 3.4 and 4.5 times higher than that in summer, winter and spring samples respectively). On the one hand, Zhang et al. (2019a, 2019b) reported that high emissions of crop residue burning were generally located in northern and northeastern China, with outstanding peaks in October. On the other hand, the concentration of K was affected by burning a large amount of coal and biomass fuels every autumn and winter in northern China. The highest of S (1485.15 ± 413.51 ng/m^3), which was a trace marker for coal combustion, was found in winter samples. It was noted that seasonal variety of the S was not significantly different, suggesting the S in Shanghai atmosphere may be contributed by other pollutant sources, such as industrial emission or vehicle emission. The highest mass level of Cl (404.09 ± 154.14 ng/m^3) was found in northwest samples, and lowest (60.81 ± 25.86 ng/m^3) in winter samples. However, Zhou et al. (2016) reported that Cl ion was higher in winter in Shanghai atmosphere. Chlorine in air can be from sea salt and anthropogenic emission. We noted that Na was near 10 times higher than that of Cl, and especially, no relationship between Na and Cl could be found. Therefore, mass level of Cl in Shanghai air not only contributed by sea salt, but also by anthropogenic emission, such as industrial emission.

The seasonal variabilities of analyzed trace elements were listed in Table 3. Average concentrations of Ti, V, Mn, Fe, Cu, Zn, Sr, and Pb in the four seasons were lower than that in previous studies (Wang et al., 2013; Ming et al., 2017).

The highest average mass level of trace elements in the $PM_{2.5}$ was Zn, its annual variable trends followed

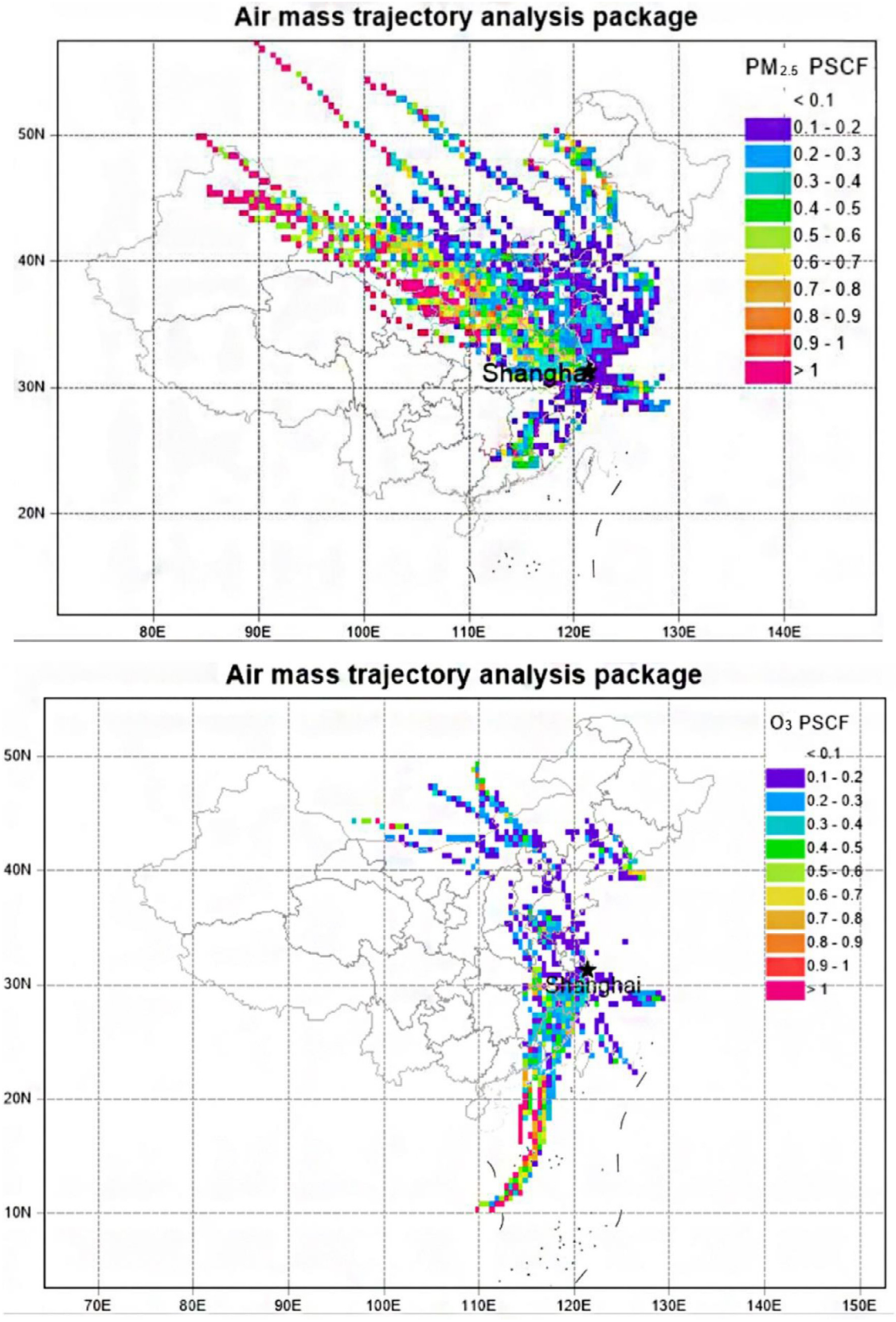

Fig. 3 – Potential source contribution function (PSCF) and concentration weighted trajectory (CWT) maps for $PM_{2.5}$ arriving at 25-m altitude at Shanghai city showing potential source regions contributing to $PM_{2.5}$ concentrations during sampling period (No. GS (2016) 1585 (http://bzdt.ch.mnr.gov.cn/index.html)).

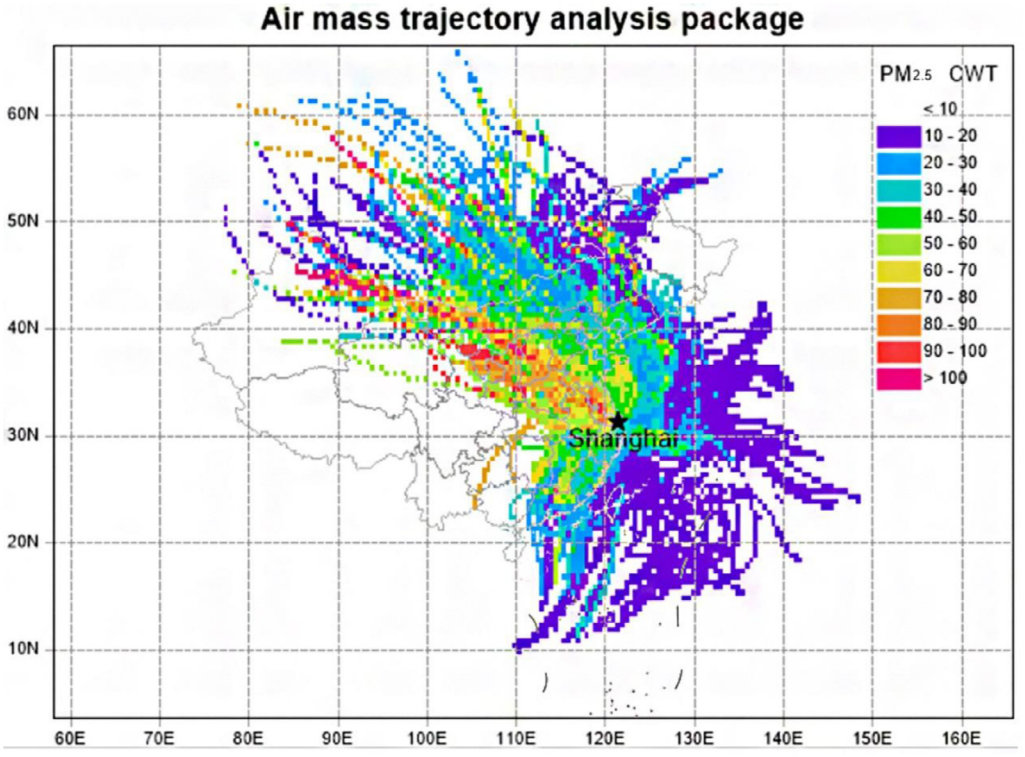

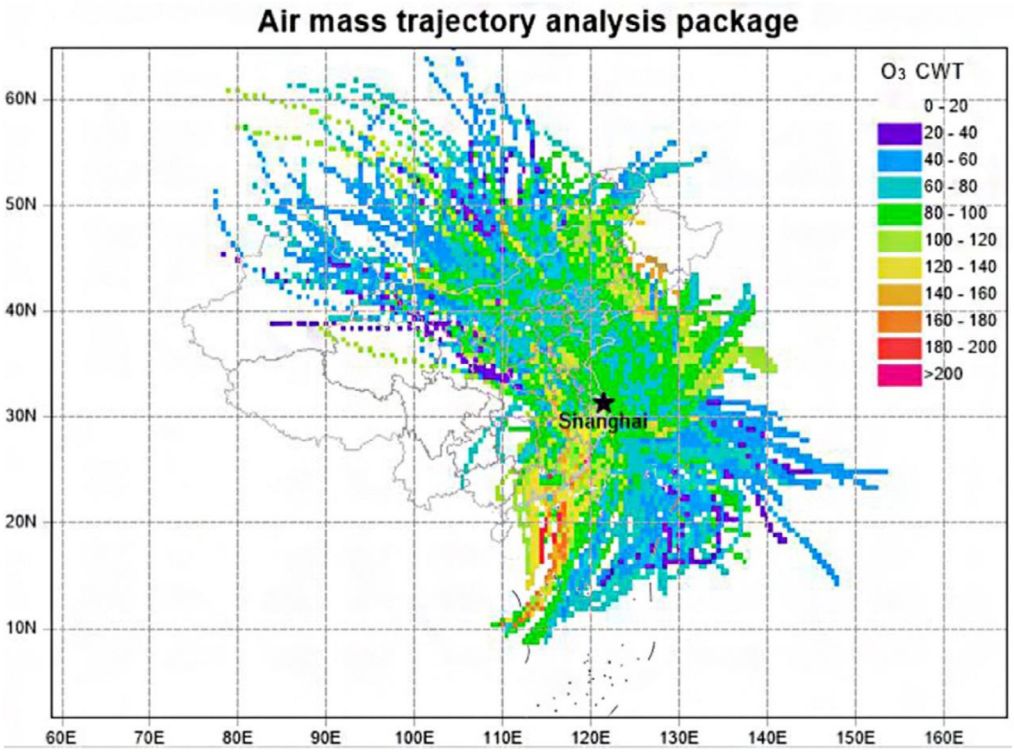

Fig. 4 – PSCF and CWT maps for O_3 arriving at 25-m altitude at Shanghai city showing potential source regions contributing to O_3 concentrations during sampling period (No. GS (2016) 1585 (http://bzdt.ch.mnr.gov.cn/index.html)).

Table 3 – Concentration (ng/m^3) of different elements in different PM2.5 sample.

Elements	Summer	Autumn/North	Winter	Spring	Northwest	r
Na	4296.77±241.18	2749.73±1152.02	355.93±249.62	580.04±233.43	3832.49±523.45	−0.26*
Mg	1461.69±19.89	1168.73±498.40	196.02±123.63	203.12±106.08	1189.41±235.51	−0.26**
Al	2662.21±185.24	2539.81±477.78	258.69±201.65	449.46±199.21	2593.37±412.35	−0.32*
P	19.68±2.96	21.22±10.43	6.69±1.46	10.80±3.24	16.98±8.11	−0.09
S	954.80±247.31	943.69±175.35	1485.15±413.51	805.39±120.66	892.76±223.44	−0.45
Cl	313.33±142.35	275.51±54.36	60.81±25.86	72.54±53.33	404.09±154.14	−0.45
K	625.42±60.06	2956.94±2415.64	868.06±80.96	661.54±67.85	940.37±232.13	−0.29
Ca	5975.16±245.84	5026.64±2620.34	824.22±90.56	385.87±299.66	6475.33±797.78	−0.43*
Ti	10.80±5.94	23.54±21.54	7.10±6.22	9.26±1.95	15.43±12.99	−0.33
V	9.57±4.30	4.63±1.89	3.47±0.67	3.34±1.80	3.01±2.40	0.30
Cr	20.07±3.24	18.21±6.20	7.10±2.31	3.70±2.31	21.61±5.61	−0.50
Mn	17.60±6.52	30.25±8.87	44.45±14.06	27.47±3.30	43.22±26.56	−0.75
Fe	310.55±93.14	417.05±128.67	456.56±131.70	350.37±31.44	572.94±282.96	−0.85
Ni	9.57±2.05	8.03±2.66	6.48±1.80	5.56±1.23	7.72±3.78	−0.22*
Cu	8.64±3.98	12.04±5.11	17.90±7.91	8.33±2.09	14.20±8.59	−0.83
Zn	31.18±24.65	73.78±22.27	142.93±45.80	79.03±11.53	104.65±64.57	−0.56
Br	5.87±1.16	8.95±0.62	16.67±5.38	12.04±2.05	12.35±6.02	−0.35
Sr	13.27±3.32	11.73±7.41	8.64±2.09	8.64±3.73	16.98±7.43	−0.51*
Ba	25.00±2.99	16.59±12.75	27.17±4.43	28.40±5.03	16.98±7.04	0.64*
Pb	8.64±6.41	18.37±6.72	41.52±10.30	24.85±3.52	38.12±28.07	−0.58
O_3	85.06±48.55	62.19±18.98	53.44±20.64	108.77±17.07	42.29±17.04	

* Correlation (r) is significant at the 0.05 level.
** Correlation (r) is significant at the 0.01 level.

the pattern, winter (142.93 ± 55.80 ng/m^3) > northwest (104.65 ± 64.57 ng/m^3) > spring (79.03 ± 11.53 ng/m^3) > autumn (73.78 ± 22.27 ng/m^3) > Summer (31.18 ± 24.65 ng/m^3). High mass concentration of Zn in ambient particles has also been reported in the atmosphere Shanghai (Lu et al., 2008, 2011). Mass level of other heavy metal elements in the fine particles ranked in the following order: Mn (32.60 ± 17.58 ng/m^3) > Pb (27.04 ± 18.64 ng/m^3) > Ba (23.09 ± 8.58 ng/m^3) > Cr (14.14 ± 8.45 ng/m^3) > Cu (12.22 ± 7.02 ng/m^3) > Sr (11.85 ± 6.14 ng/m^3) > Ni (7.47 ± 2.82 ng/m^3) > V (4.90 ± 3.60 ng/m^3). V and Ni were probably associated to fossil fuel combustion including ships and power plants (Zhang et al., 2019a, 2019b). Barium was most abundant in gasoline exhaust $PM_{2.5}$ samples (Cui et al., 2019). Cu and Zn were the markers for traffic emission sources. These elements were found in PMs because of tire wear, lubricating oil combustion, and vehicle brake abrasion (Liu et al., 2015). Mn, Cu, Zn, Pb came from industrial emission (Xue et al., 2019; Shridhar et al., 2010). The mass concentrations of Mn, Cu, Zn, and Pb were the highest in winter were contributed by the $PM_{2.5}$ carried by the air mass from northern China. The air mass covered many industrial parks in northern China. The low wind speeds (average speed was 1.2 m/sec during the sampling time) and low temperatures in winter might lead to air poor dispersion, and increased the concentrations of these species in winter $PM_{2.5}$ samples (Ancelet et al., 2014).

As the dominant species of the transition metals in the atmosphere (Zhang et al., 2014), mass concentration of iron (Fe) in ambient particles was higher than that of other trace metals. Fe in Shanghai ambient particles could be from natural sources (such as fugitive soil, dust storm) and anthropogenic sources (such as industrial process, coal combustion emissions). Its annual variety character followed the pattern, northwest (572.94 ± 282.96 ng/m^3) > winter (456.56 ± 131.70 ng/m^3) > autumn (417.05 ± 128.67 ng/m^3) > spring (350.37 ± 31.44 ng/m^3) > summer (310.55 ± 93.14 ng/m^3). Compared with the previous reports (Lu et al., 2008; Wang et al., 2013), mass level of Fe in Shanghai $PM_{2.5}$ has decreased greatly, and seasonal variety of Fe in the $PM_{2.5}$ had no significantly different.

2.5. *Correlation between ozone level and the concentration of chemical elements*

Our O_3 monitoring data showed O_3 high concentration was found in spring and summer, and low concentration in autumn and winter. The average concentration of ozone in summer, autumn, winter, and spring was 85.06 ± 48.55, 62.19 ± 18.98, 53.44 ± 20.64, and 108.77 ± 17.07 μg/m^3 respectively. It was worth noting that average mass level of O_3 from northwest samples (42.29 ± 17.04 μg/m^3) was lower than that of seasonal samples. The relationship between the ozone concentration and the chemical composition level was calculated and listed in Table 3.

The relationship data showed that the ozone concentrations had positive correlation with Ba ($r = 0.64$, $p < 0.05$) and V ($r = 0.30$, $p > 0.05$), and negative correlation with other measured chemical elements. Ba was regarded from traffic road emission (Cui et al., 2019; Luo et al., 2018), and V was associated to fossil fuel combustion (Rodríguez et al., 2004). The ozone near the ground surface was mainly formed by some complex chemical reactions between nitrogen oxides (NO_x) and volatile organic compounds (VOCs) (Wang et al., 2017). Considering that the O_3 production in Shanghai city was clearly under a VOC-limited regime, in which the aromatics and alkenes played the dominant roles (Geng et al., 2008), therefore, our data indirectly demonstrated that O_3 in Shanghai atmosphere was largely formed from VOCs. Additionally, our potential source model results showed that larger PSCF and CWT value was mainly found in Zhejiang province, Fujian province, Guangdong province and South China Sea. Zhang et al. (2019a, 2019b) reported that high O_3 level could be found when the southeastern wind (from Hangzhou Bay, Zhejiang Province and East China Sea) was dominant, this cluster could be the potential exogenous sources of high O_3.

Above all, combining the characterization of VOCs, Ba and V, high O_3 level in Shanghai atmosphere was mainly caused by the joint effect of local to regional precursor emissions and super-regional O_3 transportation.

3. Conclusions

The annual mean $PM_{2.5}$ mass concentration in Shanghai has decreased under implementation of Chinese Clean Air Action Plan since 2013. However, O_3 pollution has been continuously worsening and has become the primary air pollutant affecting the ambient air quality instead of $PM_{2.5}$ in Shanghai. Better understanding of the elevated O_3 and its potential sources is important for making policy to improve air quality. Based long term field observation of $PM_{2.5}$ and O_3, our main conclusions are summarized as follows:

(1) Our data showed that the annual average concentration of $PM_{2.5}$ and average O_3-8 hr was 39.35 ± 35.74 and 86.49 ± 41.65 μg/m^3 respectively. The concentration of $PM_{2.5}$ showed clear seasonal trends, with higher concentrations in autumn/winter and lower concentrations in spring/summer, however, the seasonal trends of O_3 was different.
(2) Air mass backward trajectory, PSCF and CWT model analyses implied that areas of northwestern China contributed significantly to the mass concentration of Shanghai $PM_{2.5}$, while pollutants from areas of eastern coastal provinces and South China Sea contributed significantly to the mass level of ozone.
(3) Ozone concentrations had good correlation with Ba ($r = 0.64$, $p < 0.05$) and V ($r = 0.30$, $p > 0.05$) suggesting the O_3 precursor (VOCs) from traffic emissions contributed to the increasing O_3 level in Shanghai atmosphere.

Declaration of competing interest

We declare that we do not have any commercial or associative interest that represents a conflict of interest in connection with the work submitted.

Acknowledgments

The National Natural Science Foundation of China (No. 21477073) for supporting us to conduct this research.

Appendix A. Supplementary data

Supplementary material associated with this article can be found in the online version at doi:10.1016/j.jes.2020.03.043.

REFERENCES

Ancelet, T., Davy, P.K., Trompetter, W.J., Markwitz, A., 2014. Sources of particulate matter pollution in a small New Zealand city. Atmos. Pollut. Res. 5 (4), 572–580.
Ashbaugh, L., Malm, W.C., Sadeh, W.Z., 1985. A residence time probability analysis of sulfur concentrations at grand Canyon National Park. Atmos. Environ. 19 (8), 1263–1270.
Cui, X., Zhou, T., Shen, Y., Rong, Y., Zhang, Z., Liu, Y., et al., 2019. Different biological effects of $PM_{2.5}$ from coal combustion, gasoline exhaust and urban ambient air relate to the PAH/metal compositions. Environ. Toxicol. Pharmacol. 69, 120–128.
Dolker, T., Agrawal, M., 2019. Negative impacts of elevated ozone on dominant species of semi-natural grassland vegetation in Indo-Gangetic plain. Ecotox. Environ. Saf. 182, 109404.
Geng, F., Tie, X., Xu, J., Zhou, G., Peng, L., Gao, W., et al., 2008. Characterizations of ozone, NOx, and VOCs measured in Shanghai, China. Atmos. Environ. 42 (29), 6873–6883.
Hsu, Y.K., Holsen, T.M., Hopke, P.K., 2003. Comparison of hybrid receptor models to locate PCB sources in Chicago. Atmos. Environ. 37 (4), 545–562.
Li, H., Wang, D., Cui, L., Gao, Y., Huo, J., Wang, X., et al., 2019a. Characteristics of atmospheric $PM_{2.5}$ composition during the implementation of stringent pollution control measures in shanghai for the 2016 G20 summit. Sci. Total Environ. 648, 1121–1129.
Li, L., An, J., Huang, L., Yan, R., Huang, C., Yarwood, G., 2019b. Ozone source apportionment over the Yangtze River Delta region, China: investigation of regional transport, sectoral contributions and seasonal differences. Atmos. Environ. 202, 269–280.
Liu, G., Li, J., Wu, D., Xu, H., 2015. Chemical composition and source apportionment of the ambient $PM_{2.5}$ in Hangzhou, China. Particuology 18, 135–143.
Lu, S., Yao, Z., Chen, X., Wu, M., Sheng, G., Fu, J., et al., 2008. The relationship between physicochemical characterization and the potential toxicity of fine particulates ($PM_{2.5}$) in Shanghai atmosphere. Atmos. Environ. 42 (31), 7205–7214.
Lu, S., Feng, M., Yao, Z., An, J., Zhong, Y., Wu, M., et al., 2011. Physicochemical characterization and cytotoxicity of ambient coarse, fine, and ultrafine particulate matters in Shanghai atmosphere. Atmos. Environ. 45 (3), 736–744.
Luo, Y., Zhou, X., Zhang, J., Xiao, Y., Wang, Z., Zhou, Y., et al., 2018. $PM_{2.5}$ pollution in a petrochemical industry city of northern China: Seasonal variation and source apportionment. Atmos. Res. 212, 285–295.
Ming, L., Jin, L., Li, J., Fu, P., Yang, W., Liu, D., et al., 2017. $PM_{2.5}$ in the Yangtze River Delta, China: Chemical compositions, seasonal variations, and regional pollution events. Environ. Pollut. 223, 200–212.
Rodrıǵuez, S., Querol, X., Alastuey, A., Viana, M., Alarcón, M., Mantilla, E., et al., 2004. Comparative PM_{10}–$PM_{2.5}$ source contribution study at rural, urban and industrial sites during PM episodes in Eastern Spain. Sci. Total Environ. 328 (1-3), 95–113.
Shridhar, V., Khillare, P.S., Agarwal, T., Ray, S., 2010. Metallic species in ambient particulate matter at rural and urban location of Delhi. J. Hazard. Mater. 175 (1-3), 600–607.
Shu, L., Wang, T., Xie, M., Li, M., Zhao, M., Zhang, M., et al., 2019. Epsiode study of fine particle and ozone during the CAPUM-YRD over Yangtze River Delta of China: characteristics and source attribution. Atmos. Environ. 203, 87–101.
Wang, J., Hu, Z., Chen, Y., Chen, Z., Xu, S., 2013. Contamination characteristics and possible sources of PM_{10} and $PM_{2.5}$ in different functional areas of Shanghai, China. Atmos. Environ. 68, 221–229.
Wang, T., Xue, L., Brimblecombe, P., Lam, Y.F., Li, L., Zhang, L., 2017. Ozone pollution in China: a review of concentrations, meteorological influences, chemical precursors, and effects. Sci. Total Environ. 575, 1582–1596.
Wang, Y., Zhang, X., Draxler, R.R., 2009. TrajStat: GIS-based software that uses various trajectory statistical analysis methods to identify potential sources from long-term air pollution measurement data. Environ. Modell. Softw. 24 (8), 938–939.
Wang, Y., Shi, Z., Shen, F., Sun, J., Huang, L., Zhang, H., et al., 2019. Associations of daily mortality with short-term exposure to PM2.5 and its constituents in Shanghai, China. Chemosphere 233, 879–887.
Xu, J., Tie, X., Gao, W., Lin, Y., Fu, Q., 2019. Measurement and model analyses of the ozone variation during 2006 to 2015 and its response to emission change in megacity Shanghai, China. Atmos. Chem. Phys. 19, 9017–9035.
Xue, H., Liu, G., Zhang, H., Hu, R., Wang, X., 2019. Similarities and differences in PM_{10} and $PM_{2.5}$ concentrations, chemical compositions and sources in Hefei City, China. Chemosphere 220, 760–765.
Zhang, G., Bi, X., Lou, S., Li, L., Wang, H., Wang, X., et al., 2014. Source and mixing state of iron-containing particles in Shanghai by individual particle analysis. Chemosphere 95, 9–16.
Zhang, J., Chen, Q., Wang, Q., Ding, Z., Sun, H., Xu, Y., 2019a. The acute health effects of ozone and $PM_{2.5}$ on daily cardiovascular disease mortality: a multi-center time series study in China. Ecotox. Environ. Safe. 174, 218–223.
Zhang, X., Lu, Y., Wang, Q., Qian, X., 2019b. A high-resolution inventory of air pollutant emissions from crop residue burning in China. Atmos. Environ. 213, 207–214.
Zhao, M., Huang, Z., Qiao, T., Zhang, Y., Xiu, G., Yu, J., 2015. Chemical characterization, the transport pathways and potential sources of $PM_{2.5}$ in Shanghai: seasonal variations. Atmos. Res. 158–159, 66–78.
Zhao, S., Yu, Y., Qin, D., Yin, D., Dong, L., He, J., 2019a. Analyses of regional pollution and transportation of $PM_{2.5}$ and ozone in the city clusters of Sichuan Basin. China Atmos. Pollut. Res. 10 (2), 374–385.
Zhao, W., Tang, G., Yu, H., Yang, Y., Wang, Y., Wang, L., et al., 2019b. Evolution of boundary layer ozone in Shijiazhuang, a suburban site on the North China Plain. J. Environ. Sci. 83, 152–160.
Zhao, T., Markevych, L., Romanos, M., Nowak, D., Heinrich, J., 2018. Ambient ozone exposure and mental health: A systematic review of epidemiological studies. Environ. Res. 165, 459–472.
Zhou, M., Qiao, L., Zhu, S., Li, L., Lou, S., Wang, H., et al., 2016. Chemical characteristics of fine particles and their impact on visibility impairment in Shanghai based on a 1-year period observation. J. Environ. Sci. 48, 151–160.